

Mariángelo Juan Ignacio Elio (Orcid ID: 0000-0002-5757-2531)

Prolonged Ca²⁺ release refractoriness and T-Tubule disruption as determinants of increased propensity to cardiac alternans in the hypertensive heart disease

Juan Ignacio Elio Mariángelo, Gabriel Darío Di Marzio, Luis Alberto Gonano, Matilde Said*, Cecilia Mundiña-Weilenmann*.

*Both are corresponding authors.

Centro de Investigaciones Cardiovasculares, CCT-CONICET La Plata, Facultad de Ciencias Médicas, Universidad Nacional de La Plata, La Plata, Argentina.

Short title: Alternans in hypertrophic myocardium

Corresponding authors:

Cecilia Mundiña-Weilenmann
Centro de Investigaciones Cardiovasculares
Facultad de Ciencias Médicas, UNLP
60 y 120, 1900 La Plata, Argentina.
Tel/Fax: 54-221-4834833
Email: cmundweil@med.unlp.edu.ar

Matilde Said
Centro de Investigaciones Cardiovasculares
Facultad de Ciencias Médicas, UNLP
60 y 120, 1900 La Plata, Argentina.
Tel/Fax: 54-221-4834833
Email: msaid@med.unlp.edu.ar

This article has been accepted for publication and undergone full peer review but has not been through the copyediting, typesetting, pagination and proofreading process which may lead to differences between this version and the [Version of Record](#). Please cite this article as doi: [10.1111/apha.13969](https://doi.org/10.1111/apha.13969)

This article is protected by copyright. All rights reserved.

ABSTRACT

Aim

Cardiac alternans is a dynamical phenomenon linked to the genesis of severe arrhythmias and sudden cardiac death. It has been proposed that alternans is caused by alterations in Ca^{2+} handling by the sarcoplasmic reticulum (SR), in both the SR Ca^{2+} uptake and release processes. The hypertrophic myocardium is particularly prone to alternans, but the precise mechanisms underlying its increased vulnerability are not known.

Methods

Mechanical alternans (intact hearts) and Ca^{2+} alternans (cardiac myocytes) were studied in spontaneously hypertensive rats (SHR) during the first year of age after the onset of hypertension and compared with age-matched normotensive rats. Subcellular Ca^{2+} alternans, T-Tubule organization, SR Ca^{2+} uptake and Ca^{2+} release refractoriness were measured.

Results

The increased susceptibility of SHR to high frequency-induced mechanical and Ca^{2+} alternans appeared when the hypertrophy developed, associated with an adverse remodelling of the T-tubule network (6 mo). At the subcellular level, Ca^{2+} discordant alternans was also observed. From 6 mo of age, SHR myocytes showed a prolongation of Ca^{2+} release refractoriness without alterations in the capacity of SR Ca^{2+} removal, measured by the frequency-dependent acceleration of relaxation. Sensitizing SR Ca^{2+} release channels (RyR2) by a low dose of caffeine or by an increase in extracellular Ca^{2+} concentration, shortened refractoriness of SR Ca^{2+} release and reduced alternans in SHR hearts.

Conclusions

The tuning of SR Ca^{2+} release refractoriness is a crucial target to prevent cardiac alternans in a hypertrophic myocardium with an adverse T-Tubule remodelling.

Key words: HYPERTENSIVE HYPERTROPHY - CARDIAC ALTERNANS - CALCIUM RELEASE REFRACTORINESS - T-TUBULE ORGANIZATION - ALTERNANS REVERSAL

INTRODUCTION

Cardiac alternans is described as beat-to-beat alternation in action potential duration, contraction strength or amplitude of Ca^{2+} transient at a constant stimulation frequency^{1,2}. Clinically, cardiac alternans is manifest as T-wave alternans, which has become an important predictor of malignant arrhythmias and sudden cardiac death³. Therefore, a better understanding of the mechanisms leading to alternans would allow for the development of appropriate antiarrhythmic strategies.

Several experimental conditions and interventions trigger the appearance of alternans which unveiled its multifactorial nature. However, evidence emerging from empirical studies and mathematical models ultimately supports that defects in intracellular Ca^{2+} handling, in particular sarcoplasmic reticulum (SR) Ca^{2+} handling, are underlying this phenomenon^{1,4-6}. The increase in intracellular Ca^{2+} that drives contraction is the result of Ca^{2+} entry through the L-type Ca^{2+} channel (LTCC) triggering the release of a larger amount of Ca^{2+} from the SR via the ryanodine receptor (RyR2). A close localization of these two proteins is ensured by the presence of a dense T-tubule (TT) network, allowing for an effective excitation-contraction coupling (ECC). Relaxation occurs when Ca^{2+} is resequenced into the SR by the Ca^{2+} pump (SERCA2a) and to a lesser extent by the efflux of Ca^{2+} through Na- Ca^{2+} exchanger (NCX). These Ca^{2+} movements should be efficient and temporarily synchronized but when the stimulation rate increases, the capacity of the myocyte to cycle Ca^{2+} is overwhelmed. This insufficient capacity has been linked to the genesis of cardiac alternans, which typically develops at faster heart rate². However the impaired Ca^{2+} dynamics present in various types of cardiac diseases, leads to the appearance of alternans at lower frequencies with the consequent increased risk of lethal arrhythmias^{7,8}.

Two main mechanisms have been proposed to be involved in the genesis of Ca^{2+} alternans: slow recovery from refractoriness of SR Ca^{2+} release or beat-to-beat fluctuations in the SR Ca^{2+} content requiring a steep SR Ca^{2+} load-release relationship together with a slow SR Ca^{2+} reuptake^{5,6,9-12}. These alterations can occur in localized regions within the myocyte giving rise to subcellular Ca^{2+} alternans or microalternans^{2,4,13}.

Left ventricular hypertrophy (LVH) is one of the earliest cardiovascular alterations produced by hypertension, and it is recognized as an independent risk factor for cardiovascular disease¹⁴. The spontaneously hypertensive rat (SHR) is a well-established model of genetic hypertension which resembles the natural evolution of the human essential hypertension¹⁵. Among other complications the hypertrophied myocardium of SHR shows an increased susceptibility for the development of Ca²⁺ alternans¹⁶⁻¹⁹. Although alterations in the ECC have been demonstrated at very early stages in SHR hearts^{20,21}, the mechanisms responsible for the premature appearance of alternans are not fully understood. We followed the progression of the hypertensive disease in SHR in order to dissect the molecular basis underlying its increased vulnerability of arrhythmogenic cardiac alternans.

RESULTS

Increased susceptibility to alternans in hypertrophied hearts of SHR

To study the occurrence of alternans in the hypertrophied myocardium, isolated Langendorff-perfused hearts from SHR 3, 6 and 12 mo of age were stimulated at increasing pacing rates and compared with age-matched normotensive rats (W). In accordance with our previous results²¹ as early as 3 mo, SHR showed increased blood pressure and myocardial hypertrophy when compared to W, conditions that remained until 12 mo of age (Figure 1S).

Figure 1A shows representative recordings of left ventricular developed pressure (LVDP) in W and SHR hearts stimulated at 4 Hz (basal) and 8.5 Hz. At all ages and in both strains, the frequency challenge produced a negative force-frequency relationship depicted by the decrease in LVDP. This response was more pronounced in SHR hearts. In 6 and 12 mo SHR hearts, the high frequency induced mechanical alternans which sustained during the whole time period the stimulation was applied. This behaviour was neither observed in age-matched W hearts nor in 3 mo hearts of both strains.

The magnitude of mechanical alternans, quantified as the alternans ratio (AR), at successive increments in stimulation frequency is shown in Figure 1B. The frequency threshold for the appearance of alternans was 11 Hz for W hearts at all ages and for 3 mo SHR hearts. For 6 and 12 mo SHR hearts, this frequency was lower (8.5 Hz). Moreover, the magnitude of the SHR AR was always higher than W AR. These results indicate an increased propensity to mechanical alternans in 6 and 12 mo SHR hearts.

The alternans vulnerability of SHR hearts was also explored at the level of isolated myocytes by measuring intracellular Ca^{2+} . Figure 2A depicts typical Ca^{2+} transient traces of 12 mo W and SHR myocytes obtained at basal frequency (0.5Hz) and after the steady state was reached at progressively increasing stimulation frequencies. The representative records show that SHR myocytes required a lower frequency to begin to alternate than W myocytes. The overall results of pacing threshold to Ca^{2+} alternans are shown in Figure 2B. At 6 and 12 mo, SHR myocytes evidenced a decreased threshold when compared to age-matched W myocytes.

The results obtained at intracellular Ca^{2+} level, confirmed a greater rate-sensitivity to alternans development of SHR myocytes.

It has been proposed that microscopic Ca^{2+} alternans represents an early manifestation of global Ca^{2+} alternans^{13,22}. To analyse subcellular Ca^{2+} dynamics we use line-scan confocal microscopy. Figure 3A shows representative line-scan images and Ca^{2+} intensity profiles of 12 mo W and SHR myocytes paced at 1 and 4 Hz. When stimulated at 4 Hz, SHR myocytes exhibited disorders in the Ca^{2+} signal which translate in Ca^{2+} alternans. Different cell zones alternate out-of-phase suggesting different availability of SR Ca^{2+} release units. This subcellular alternans, known as discordant alternans, was quantified by the discordance index (Figure 3B). The index value at 4 Hz was significantly increased in SHR when compared to aged-matched W myocytes.

Since T-tubule structure is an important determinant of the synchrony of SR Ca^{2+} release²³⁻²⁵, we next investigated if TT network heterogeneities were underlying the subcellular impairment in Ca^{2+} handling and the premature appearance of Ca^{2+} alternans in SHR myocytes. TT density, measured by confocal microscopy, was not different in 3 mo SHR myocytes when compared to W myocytes. However, 6 and 12 mo SHR myocytes showed a structural remodelling of the TT system, with TT loss at discrete and local regions in comparison with age-matched W myocytes. Typical confocal images of 6 mo myocytes are shown in Figure 4A. The peak power value, used as a quantitative index of TT integrity, decreased in SHR myocytes (Figure 4B). Moreover, a further analysis of the geometrical organization of the TT system revealed a greater fraction of longitudinal vs. transverse components in SHR myocytes (Figure 4C). This rearrangement was not associated with changes in the expression of caveolin-3 and junctophilin-2, two proteins involved in the structure and maintenance of the T-tubule system (Figure 2S).

Role of SR in determining Ca^{2+} alternans in SHR myocytes

It has been reported that alterations in SR function can underlie the initiation of Ca^{2+} alternans^{4,10,11,26,27}. We next investigated if modifications in SR Ca^{2+} uptake and/or release were involved in determining the greater propensity to Ca^{2+} alternans of SHR myocytes. To study the contribution of SR Ca^{2+} uptake we evaluated the frequency-dependent acceleration of relaxation of the Ca^{2+} transient (FDAR). FDAR relies on the fact that

SERCA2a-mediated SR Ca^{2+} uptake increases at higher frequencies, a physiological mechanism that ensures proper ventricular diastolic filling with increasing heart rates. Myocytes were simulated at 0.5 Hz (basal) and 3 Hz, a frequency at which Ca^{2+} alternans was normally absent in both strains. Ca^{2+} transient decline was faster at 3 Hz than at 0.5 Hz in W as well as in SHR myocytes (Figure 5A). The average data shows that the magnitude of the high frequency-induced decrease in the time constant of the single exponential decay of Ca^{2+} transient (τ) was similar in W and SHR myocytes, suggesting that SR Ca^{2+} uptake was not impaired in 6 and 12 mo SHR myocytes (Figure 5B). Similar results were observed with the frequency-induced relaxant effect measured by the decrease in half relaxation time ($t_{1/2}$) in intact hearts (Figure 3S).

An alternative cellular mechanism potentially involved in the genesis of Ca^{2+} alternans is the rate of SR Ca^{2+} release recovery, known as refractoriness^{11,26,27}. To investigate this mechanism, we compared refractoriness of SR Ca^{2+} release in myocytes from W and SHR applying premature electrical pulses at different time intervals during the regular pacing-induced Ca^{2+} transients. Figure 6A shows typical recordings of cytosolic Ca^{2+} transients at various S1-S2 coupling intervals from 6 mo W and SHR myocytes. The average restitution curve of SR Ca^{2+} release was significantly right-shifted (Figure 6B) and the time interval to 50% recovery increased in SHR myocytes when compared to W myocytes (Figure 6C), indicating a slowing in the recovery of SR Ca^{2+} release. Similar results were observed in 12 mo myocytes (Figure 4S). Caffeine at low dose, which has been used to enhance RyR2 activity by reducing the threshold for luminal Ca^{2+} activation²⁸, was able to accelerate the recovery of SR Ca^{2+} release in SHR myocytes (Figure 6B and 6C). Furthermore, caffeine also rescued SHR myocytes from high frequency-induced alternans (Figure 6D) and reduced the Ca^{2+} AR (Figure 6E). Treatment with caffeine also suppressed mechanical alternans in perfused SHR hearts (Figure 5S A and B).

We next explore whether cardiac alternans in SHR hearts can be overcome by increasing extracellular Ca^{2+} concentration. It has been shown that duplicating normal extracellular Ca^{2+} concentration in mice myocytes enhances SR Ca^{2+} content without changing diastolic Ca^{2+} , thus favouring RyR2 opening by the increase in SR luminal Ca^{2+} ²⁹. We confirmed that in 6 mo SHR myocytes, increasing extracellular Ca^{2+} concentration in the perfusion buffer from 1 mM to 2.5 mM, enhanced SR Ca^{2+} content without modifying diastolic Ca^{2+} (Figure 7A and B). This enhancement in extracellular Ca^{2+} shortened Ca^{2+} release refractoriness and reduced the time to

50% recovery of Ca^{2+} release (Figure 7C and D), alleviating Ca^{2+} alternans (Figure 7E) and decreasing Ca^{2+} AR (Figure 7F). Increasing extracellular Ca^{2+} also suppressed mechanical alternans in perfused SHR hearts (Figure 5S C and D). The fact that both caffeine and the increase in extracellular Ca^{2+} concentration corrected the abnormal refractoriness of Ca^{2+} release and effectively suppressed the premature appearance of mechanical and Ca^{2+} alternans in SHR, allow us to propose that the prolonged refractoriness of SR Ca^{2+} release is a key determinant of the greater susceptibility to alternans of aged SHR.

DISCUSSION

Cardiac alternans is recognized as an important substrate for life-threatening arrhythmias. In the present study, we investigated the susceptibility to cardiac alternans and the mechanisms involved in its appearance in the SHR model during the first year of age after the onset of hypertension. The results demonstrate that SHR hearts from 6 mo of age showed an increased vulnerability to mechanical, global and subcellular Ca^{2+} alternans when compared with age-matched normotensive rats. The appearance of an earlier onset of alternans occurs associated with a structural modification of the TT membrane system and an increased refractoriness of SR Ca^{2+} release, with no significant differences in the speed of SR Ca^{2+} uptake.

Consistently with previous studies from our laboratory, cardiac hypertrophy was present shortly after the development of hypertension in the SHR model (3 mo of age)²¹ and the level of hypertrophy did not differ from that observed at older ages (6 and 12 mo). However, a lower threshold for cardiac alternans appeared only when the hypertrophy occurred associated with a remodeling of the TT system. The TT remodeling included a decreased regularity of the transverse organization and an increased fraction of longitudinally oriented elements, a feature observed in immature and failing cardiomyocytes, which has been associated to an impaired of critical excitation-contraction Ca^{2+} handling mechanisms^{30,31}.

Cardiac alternans is known to occur when heart rate exceeds the ability of the cells to effectively handle intracellular Ca^{2+} , being the SR Ca^{2+} cycling the major rate-limiting process^{2,3}. During Ca^{2+} alternans the amount of Ca^{2+} released by the SR alternates on beat-to-beat basis. This could be due to either oscillations in the SR Ca^{2+} content or an increased refractoriness of SR Ca^{2+} release. These two mechanisms, that are not mutually exclusive, can acquire different relevance as precursors of alternans, depending on: pathophysiological conditions, cell type (atrial vs. ventricular cells) and temperature^{5,18,32,33}.

SR Ca^{2+} release refractoriness is a complex phenomenon primarily governed by RyR2 properties such as luminal Ca^{2+} modulation, Ca^{2+} -calmodulin dependent inactivation, phosphorylation, and oxidation, among others³⁴.

Abnormalities in SR Ca^{2+} release refractoriness is an important factor determining different types of arrhythmic substrates. An abbreviated refractoriness leads to the appearance of Ca^{2+} triggered arrhythmias while a prolongation has been associated to Ca^{2+} alternans. Ablation and mutations of calsequestrin -a direct regulator

of luminal Ca^{2+} modulation of RyR2-, CaMKII-dependent phosphorylation, oxidation and gain-of-function mutations of RyR2 have been described to shorten SR Ca^{2+} release refractoriness, promoting Ca^{2+} waves, delayed afterdepolarizations and triggered arrhythmias in the setting of catecholaminergic polymorphic ventricular tachycardia and heart failure^{26,35-38}. On the other hand, loss-of-function mutations of RyR2 and interventions such as tetracaine, intracellular acidification and metabolic inhibition, that decrease RyR2 activity, prolonged SR Ca^{2+} release refractoriness and enhanced propensity for Ca^{2+} alternans³⁹⁻⁴². The slowed recovery from refractoriness of SR Ca^{2+} release detected in 6 and 12 mo SHR myocytes in the present experiments could be the result of an unknown alteration of intrinsic properties of RyR2 or the consequence of the disruption of the TT system. At low TT density, a lower number of RyR2 can be directly activated by LTCC leaving orphaned RyR2, which can be later activated by Ca^{2+} released from neighbouring RyR2²⁵. Nivala et al.⁴³ using a mathematical model showed that under these conditions, refractoriness of SR Ca^{2+} release is the primary mechanism for alternans development and TT disruption could lead to Ca^{2+} alternans even in the absence of the dysfunction of Ca^{2+} handling proteins. Our results are in line with these findings. SERCA2a function in SHR hearts is not altered, as suggested by the conserved FDAR, and no modifications in the expression of major Ca^{2+} handling proteins were observed in the SHR model within the age range studied²¹. A slowed restitution of SR Ca^{2+} release in association with an increased vulnerability to Ca^{2+} alternans was shown by Kapur et al.¹⁶ in the SHR model at 7.5 and 9 mo. However, these alterations were not studied early in the hypertrophied myocardium of SHR and no examination of TT network was simultaneously performed. We showed that the greater susceptibility to mechanical and Ca^{2+} alternans is already present in 6 mo SHR hearts together with the prolongation in the SR Ca^{2+} release refractoriness and a remodelling of the TT system. In agreement with our results, Mitsuyama et al.⁴⁴ have shown an increased susceptibility to Ca^{2+} alternans in the SHR model at 18-24 weeks. However, they attributed this finding to the activation of Ca^{2+} calmodulin dependent protein kinase (CaMKII). Our previous results showed that CaMKII is indeed activated in the SHR hearts²¹, however this activation is present from 3 mo of age, time at which in the current experiments no increased susceptibility to alternans was detected.

In order to prevent pacing-induced mechanical and Ca^{2+} alternans in SHR hearts we used two interventions: an acute sensitization of RyR2 by a low dose of caffeine and an increase in extracellular Ca^{2+} . These two manoeuvres were able to shorten the refractoriness of SR Ca^{2+} release and to reduce the alternans ratio in SHR myocytes. While caffeine induced these effects under normal or low SR Ca^{2+} content⁴⁵, the beneficial effects of the enhancement of extracellular Ca^{2+} occurred with an increase in SR Ca^{2+} content. Therefore, improvement of SR Ca^{2+} release refractoriness in the presence of TT disruption, independently of SR Ca^{2+} load, is sufficient to alleviate cardiac alternans in a well-established hypertrophic myocardium. It has been reported that increments in extracellular Ca^{2+} can either attenuate or aggravate mechanical and Ca^{2+} alternans^{33,46}. In our conditions when we further increased extracellular Ca^{2+} from 1.35 to 5 or 7.5 mM, severe arrhythmias such as tachycardia and fibrillation were observed (data not shown).

Overall, the novelty of our findings was to point out that the improvement of SR Ca^{2+} release refractoriness is determinant in alleviating Ca^{2+} alternans in the SHR hypertrophic myocardium, even in the presence of TT disruption. Our results indicate the potential utility of targeting the tuning of SR Ca^{2+} release refractoriness for the treatment of cardiac alternans, which is considered a strong predictor of severe arrhythmias and sudden cardiac death.

MATERIALS & METHODS

Animals

Experiments were performed in male SHR and age-matched normotensive Wistar rats of 3, 6 or 12 months (mo) of age (200-450 g body weight). Echocardiographic characterization of both strains was previously performed²¹. Animals were inbred and maintained in our animal facilities in accordance with the Guide for the Care and Use of Laboratory Animals. The protocols were approved by the Institutional Animal Care and Use Committee (CICUAL) of School of Medicine, National University of La Plata, Argentina (Nro T05022014). Rats were anticoagulated (heparin 2.5 units/g body weight) and anesthetized with urethane (i.p. 1.2-1.4 g/kg). After phase III of anesthesia was reached, hearts were immediately removed and mounted in a Langendorff apparatus.

Ex vivo experiments: intact hearts

Isolated hearts were perfused at constant temperature (37°C), heart rate (4Hz) and flow (14 ml/min) with a buffer solution containing (in mM): 128.3 NaCl, 4.7 KCl, 1.35 CaCl₂, 20.2 NaHCO₃, 0.4 NaH₂PO₄, 1.1 MgSO₄, 11.1 glucose and 0.04 Na₂EDTA (pH adjusted to 7.4 with 95% O₂-5% CO₂), as previously described⁴⁷. A balloon connected to a pressure transducer (ADInstruments MLT 0380, CO, USA) was introduced to the left ventricle (LV) to assess mechanical activity. The balloon was filled with aqueous solution to an end diastolic pressure (LVEDP) of 5-10 mmHg. LV contractility was evaluated using the developed-pressure (LVDP) and relaxation was assessed by half relaxation time ($t_{1/2}$).

Myocytes isolation

Myocytes were isolated by enzymatic digestion as previously described⁴⁸. Briefly excised hearts were perfused at 37 °C with HEPES Buffer Solution (HBS) containing (in mM): 146.2 NaCl, 4.7 KCl, 1.0 CaCl₂, 10.0 HEPES, 0.35 NaH₂PO₄, 1.05 MgSO₄, 10.0 glucose (pH adjusted to 7.4 with NaOH). The solution was continuously bubbled with 100% O₂. After a stabilization, hearts were perfused with nominally Ca²⁺-free HBS solution with 0.1 mM EGTA for 4 min, then proceeded with added collagenase (130-145 U/mL) and 1% bovine serum albumin (BSA), in HBS containing 50 μM CaCl₂ until the heart became flaccid (15-25 min). They were then removed from the perfusion apparatus and the desegregated myocytes were separated from the undigested tissue and rinsed

several times with a HBS solution containing 1% BSA and 50 μM CaCl_2 . Ventricular myocytes were allowed to sediment several times while extracellular Ca^{2+} concentration was progressively increased to 1 mM. Only rod-shaped myocytes showing clear striations and contraction in response to electrical stimulation, were used. Cell capacitance, as an index of total surface area, and cross-sectional area were enlarged in SHR myocytes when compared to W myocytes⁴⁹.

Intracellular Ca^{2+} measurements

Isolated myocytes were loaded with Fura-2-AM (5 $\mu\text{mol/L}$ for 15 min) (Invitrogen). After removal of residual extracellular dye by centrifugation, intracellular Ca^{2+} was measured with an epifluorescence system (Ion Optix Corp., Milton, MA, USA). Myocytes were placed in a chamber on the stage of an inverted microscope (Nikon TE 2000-U), superfused at a constant flow (1 mL/min) and stimulated via two-platinum electrodes on either side of the cell bath (0.5 Hz-5Hz). Experiments were performed at room temperature (20-22°C). Intracellular Ca^{2+} was assessed from the ratio of the Fura-2 fluorescence at 510 nm in response to alternate excitation at 340 and 380 nm. Data were stored and analyzed using IonWizard software (IonOptix Corp., Milton, MA, USA). Average of 10-15 Ca^{2+} transients for each time period was used for analysis. Ca^{2+} transient amplitude, time constant of Ca^{2+} transient decay (Tau) and diastolic Ca^{2+} were measured. Figure 6S shows these parameters at 3, 6 and 12 mo in both stains at basal frequency (0.5 Hz).

SR Ca^{2+} content was assessed by rapid application of 50 mM caffeine as previously described²¹.

Alternans protocol

Cardiac alternans was induced by incrementally increasing the pacing frequency (4-11 Hz in isolated hearts, 0.5-6 Hz in isolated myocytes). The minimal frequency that produces stable alternans, sustained for at least 30 sec, was considered as threshold. The degree of alternans was quantified as the ratio (large - short/large) where large and short are the amplitudes of LVDP or Ca^{2+} transient of two consecutive stimulations in isolated hearts and myocytes respectively. The presence of alternans was considered when the alternans ratio (AR) was higher than 0.1. Low doses of caffeine (100 μM) and high extracellular Ca^{2+} concentration (2.5 mM) were tested for their ability to reverse alternans.

Restitution protocol

Restitution curves were obtained by applying premature electrical pulses (S2) at different times with respect to the regular pacing pulses (S1) (Figure 6A). The kinetics of the recovery of Ca^{2+} transients was analyzed by changing the time interval between electrical stimulations (S1-S2). Fractional recovery ratios ($\%A2/A1$), where A2 and A1 are amplitudes of Ca^{2+} transient at S2 and S1 respectively, were plotted as function of the time interval (S2-S1). The time interval to 50% of recovery of Ca^{2+} transient was calculated.

Detection of cytosolic Ca^{2+} by confocal microscopy

W o SHR ventricular myocytes were loaded with Fluo-4-AM (10 μM for 10 min) (Invitrogen). Cells were mounted in a chamber placed into an inverted microscope equipped with a 63 \times 1.4NA objective, superfused at constant flow (1 mL/min) and stimulated at 0.5-5 Hz. After a stabilization of 3-5 min, confocal line-scan images (512 \times 512 pixels/frame) at a speed of 4.3 ms/line were collected along the longitudinal axis of myocytes, avoiding nuclei, using a Zeiss LSM 410 confocal system (Axiovert 100). The fluorescent dye was excited at 488 nm (argon laser) and emissions were collected at 500-550 nm.

To determine the discordance index (DI), a region of interest (ROI) of 66 μm was manually selected within each cell and maintained in subsequent images taken from the same cell. Within this ROI, local Ca^{2+} transients were defined by dividing the line-scan into narrow regions (2 μm), which corresponds approximately to the size of an individual CRU^{24,50}. Amplitudes of two consecutive local Ca^{2+} transients were used to determine local AR and DI was calculated as the standard deviation of AR values for 33 local Ca^{2+} transients per image.

Cell membrane and T-tubular system imaging

Isolated myocytes were loaded with di-8-aminonaphthylethylpyridinium (Di-8-ANNEPS, Molecular Probes) (5 μM for 10 min). The fluorescent probe was excited at 488 nm with an argon laser and emission was collected at 560 nm. In Di-8-ANNEPS-stained myocytes, quantitative analysis of T-tubular organization was performed using the TTorg plugin for ImageJ⁵². Cardiomyocyte size and the fraction of transverse and longitudinal oriented elements of the T-tubule system were calculated using the program Tubulator⁵³. Cardiomyocyte area was significantly greater in SHR group (5431.16 \pm 509 μm^2 vs. 985.94 \pm 270 μm^2 , n=33/4 and 17/2 for 6 mo SHR and W respectively).

Statistics

Data are expressed as mean \pm SEM. Statistical significance was determined by Student's test for paired or unpaired observations as appropriate, and ANOVA when different groups were compared. The Newman-Keuls test was used to examine statistical differences observed with the ANOVA. A P value <0.05 was considered statistically significant.

Accepted Article

ACKNOWLEDGEMENTS

We would like to thank Dr. Leticia Vittone for extensively reviewing the manuscript and Dr. Margarita Salas for her precious help in editing the manuscript. This work was supported by Agencia Nacional de Promoción Científica y Tecnológica, Argentina (PICT-2018-02553 to C. Mundiña-Weilenmann) and by Consejo de Investigaciones Científicas y Técnicas (CONICET), Argentina (PIP # 0507 to C. Mundiña-Weilenmann). The authors are grateful for the excellent technical assistance of Mónica Rando, Lucía Pagola and Leandro Di Cianni.

CONFLICTS OF INTEREST

No conflicts of interest, financial or otherwise, are declared by the authors.

Fundings: This work was supported by Agencia Nacional de Promoción Científica y Tecnológica, Argentina (PICT-2018-02553 to C. Mundiña-Weilenmann) and by Consejo de Investigaciones Científicas y Técnicas (CONICET), Argentina (PIP #0507 to C. Mundiña-Weilenmann).

REFERENCES

1. Laurita KR, Rosenbaum DS. Cellular mechanisms of arrhythmogenic cardiac alternans. *Prog Biophys Mol Biol.* 2008;97(2-3):332-347.
2. Qu Z, Nivala M, Weiss JN. Calcium alternans in cardiac myocytes: order from disorder. *J Mol Cell Cardiol.* 2013;58:100-109.
3. Cutler MJ, Rosenbaum DS. Explaining the clinical manifestations of T wave alternans in patients at risk for sudden cardiac death. *Heart rhythm.* 2009;6(3 Suppl):S22-28.
4. Aistrup GL, Shiferaw Y, Kapur S, Kadish AH, Wasserstrom JA. Mechanisms underlying the formation and dynamics of subcellular calcium alternans in the intact rat heart. *Circ Res.* 2009;104(5):639-649.
5. Lugo CA, Cantalapiedra IR, Penaranda A, Hove-Madsen L, Echebarria B. Are SR Ca content fluctuations or SR refractoriness the key to atrial cardiac alternans?: insights from a human atrial model. *Am J Physiol Heart Circ Physiol.* 2014;306(11):H1540-1552.
6. Nivala M, Qu Z. Calcium alternans in a couplon network model of ventricular myocytes: role of sarcoplasmic reticulum load. *Am J Physiol Heart Circ Physiol.* 2012;303(3):H341-352.
7. Chang KC, Bayer JD, Trayanova NA. Disrupted calcium release as a mechanism for atrial alternans associated with human atrial fibrillation. *PLoS Comput Biol.* 2014;10(12):e1004011.
8. Narayan SM, Franz MR, Clopton P, Pruvot EJ, Krummen DE. Repolarization alternans reveals vulnerability to human atrial fibrillation. *Circulation.* 2011;123(25):2922-2930.
9. Alvarez-Lacalle E, Cantalapiedra IR, Penaranda A, Cinca J, Hove-Madsen L, Echebarria BJPo. Dependency of calcium alternans on ryanodine receptor refractoriness. 2013;8(2):e55042.
10. Díaz ME, O'Neill SC, Eisner DA. Sarcoplasmic reticulum calcium content fluctuation is the key to cardiac alternans. *Circ Res.* 2004;94(5):650-656.
11. Shkryl VM, Maxwell JT, Domeier TL, Blatter LA. Refractoriness of sarcoplasmic reticulum Ca²⁺ release determines Ca²⁺ alternans in atrial myocytes. *Am J Physiol Heart Circ Physiol.* 2012;302(11):H2310-2320.

12. Wang L, Myles RC, De Jesus NM, Ohlendorf AK, Bers DM, Ripplinger CM. Optical mapping of sarcoplasmic reticulum Ca²⁺ in the intact heart: ryanodine receptor refractoriness during alternans and fibrillation. *Circ Res*. 2014;114(9):1410-1421.
13. Tian Q, Kaestner L, Lipp P. Noise-free visualization of microscopic calcium signaling by pixel-wise fitting. *Circ Res*. 2012;111(1):17-27.
14. Kannel WB. Left ventricular hypertrophy as a risk factor: the Framingham experience. *J Hypertens Suppl*. 1991;9(2):S3-8; discussion S8-9.
15. Doggrell SA, Brown LJC. Rat models of hypertension, cardiac hypertrophy and failure. 1998;39(1):89-105.
16. Kapur S, Aistrup GL, Sharma R, et al. Early development of intracellular calcium cycling defects in intact hearts of spontaneously hypertensive rats. *Am J Physiol Heart Circ Physiol*. 2010;299(6):H1843-1853.
17. Nguyen TP, Sovari AA, Pezhouman A, et al. Increased susceptibility of spontaneously hypertensive rats to ventricular tachyarrhythmias in early hypertension. *J Physiol*. 2016;594(6):1689-1707.
18. Pluteanu F, Hess J, Plackic J, et al. Early subcellular Ca²⁺ remodelling and increased propensity for Ca²⁺ alternans in left atrial myocytes from hypertensive rats. *Cardiovasc Res*. 2015;106(1):87-97.
19. Wasserstrom JA, Sharma R, Kapur S, et al. Multiple defects in intracellular calcium cycling in whole failing rat heart. *Circ Heart Fail*. 2009;2(3):223-232.
20. Dupont S, Maizel J, Mentaverri R, et al. The onset of left ventricular diastolic dysfunction in SHR rats is not related to hypertrophy or hypertension. 2012;302(7):H1524-H1532.
21. Rodriguez JS, Velez Rueda JO, Salas M, et al. Increased Na⁺/Ca²⁺ exchanger expression/activity constitutes a point of inflection in the progression to heart failure of hypertensive rats. *PLoS One*. 2014;9(4):e96400.
22. Veasy J, Lai YM, Coombes S, Thul R. Complex patterns of subcellular cardiac alternans. *J Theor Biol*. 2019;478:102-114.
23. Guo A, Zhang C, Wei S, Chen B, Song L-S. Emerging mechanisms of T-tubule remodelling in heart failure. *Cardiovascular Research*. 2013;98(2):204-215.

24. Louch WE, Bito V, Heinzel FR, et al. Reduced synchrony of Ca²⁺ release with loss of T-tubules—a comparison to Ca²⁺ release in human failing cardiomyocytes. *Cardiovasc Res*. 2004;62(1):63-73.
25. Song L-S, Sobie EA, McCulle S, Lederer W, Balke CW, Cheng HJ PotNAoS. Orphaned ryanodine receptors in the failing heart. 2006;103(11):4305-4310.
26. Kornyejev D, Petrosky AD, Zepeda B, Ferreiro M, Knollmann B, Escobar AL. Calsequestrin 2 deletion shortens the refractoriness of Ca²⁺(+) release and reduces rate-dependent Ca²⁺(+)-alternans in intact mouse hearts. *J Mol Cell Cardiol*. 2012;52(1):21-31.
27. Picht E, DeSantiago J, Blatter LA, Bers DM. Cardiac alternans do not rely on diastolic sarcoplasmic reticulum calcium content fluctuations. *Circ Res*. 2006;99(7):740-748.
28. Kong H, Jones PP, Koop A, Zhang L, Duff HJ, Chen SWJBJ. Caffeine induces Ca²⁺ release by reducing the threshold for luminal Ca²⁺ activation of the ryanodine receptor. 2008;414(3):441-452.
29. Cely-Ortiz A, Felice JI, Díaz-Zegarra LA, et al. Determinants of Ca²⁺ release restitution: Insights from genetically altered animals and mathematical modeling. 2020;152(11).
30. Lipsett DB, Frisk M, Aronsen JM, et al. Cardiomyocyte substructure reverts to an immature phenotype during heart failure. *J Physiol*. 2019;597(7):1833-1853.
31. Setterberg IE, Le C, Frisk M, Perdreau-Dahl H, Li J, Louch WE. Corrigendum: The Physiology and Pathophysiology of T-Tubules in the Heart. *Front Physiol*. 2021;12:790227.
32. Cutler MJ, Wan X, Laurita KR, Hajjar RJ, Rosenbaum DS. Targeted SERCA2a gene expression identifies molecular mechanism and therapeutic target for arrhythmogenic cardiac alternans. *Circ Arrhythm Electrophysiol*. 2009;2(6):686-694.
33. Millet J, Aguilar-Sanchez Y, Kornyejev D, et al. Thermal modulation of epicardial Ca²⁺ dynamics uncovers molecular mechanisms of Ca²⁺ alternans. 2021;153(2).
34. Györke S, Belevych AE, Liu B, Kubasov IV, Carnes CA, Radwański PB. The role of luminal Ca regulation in Ca signaling refractoriness and cardiac arrhythmogenesis. *J Gen Physiol*. 2017;149(9):877-888.

35. Belevych AE, Terentyev D, Terentyeva R, et al. Shortened Ca²⁺ signaling refractoriness underlies cellular arrhythmogenesis in a postinfarction model of sudden cardiac death. *Circ Res*. 2012;110(4):569-577.
36. Brunello L, Slabaugh JL, Radwanski PB, et al. Decreased RyR2 refractoriness determines myocardial synchronization of aberrant Ca²⁺ release in a genetic model of arrhythmia. *Proc Natl Acad Sci U S A*. 2013;110(25):10312-10317.
37. Liu N, Denegri M, Dun W, et al. Abnormal propagation of calcium waves and ultrastructural remodeling in recessive catecholaminergic polymorphic ventricular tachycardia. *Circ Res*. 2013;113(2):142-152.
38. Paavola J, Viitasalo M, Laitinen-Forsblom PJ, et al. Mutant ryanodine receptors in catecholaminergic polymorphic ventricular tachycardia generate delayed afterdepolarizations due to increased propensity to Ca²⁺ waves. *European heart journal*. 2007;28(9):1135-1142.
39. Díaz ME, Eisner DA, O'Neill SC. Depressed ryanodine receptor activity increases variability and duration of the systolic Ca²⁺ transient in rat ventricular myocytes. *Circ Res*. 2002;91(7):585-593.
40. Hüser J, Wang YG, Sheehan KA, Cifuentes F, Lipsius SL, Blatter LA. Functional coupling between glycolysis and excitation-contraction coupling underlies alternans in cat heart cells. *J Physiol*. 2000;524 Pt 3(Pt 3):795-806.
41. Sun B, Wei J, Zhong X, et al. The cardiac ryanodine receptor, but not sarcoplasmic reticulum Ca(2+)-ATPase, is a major determinant of Ca(2+) alternans in intact mouse hearts. *J Biol Chem*. 2018;293(35):13650-13661.
42. Zhong X, Sun B, Vallmitjana A, et al. Suppression of ryanodine receptor function prolongs Ca²⁺ release refractoriness and promotes cardiac alternans in intact hearts. *The Biochemical journal*. 2016;473(21):3951-3964.
43. Nivala M, Song Z, Weiss JN, Qu Z. T-tubule disruption promotes calcium alternans in failing ventricular myocytes: mechanistic insights from computational modeling. *J Mol Cell Cardiol*. 2015;79:32-41.

44. Mitsuyama H, Yokoshiki H, Watanabe M, Mizukami K, Shimokawa J, Tsutsui H. Ca²⁺/calmodulin-dependent protein kinase II increases the susceptibility to the arrhythmogenic action potential alternans in spontaneously hypertensive rats. *Am J Physiol Heart Circ Physiol*. 2014;307(2):H199-206.
45. Trafford AW, Díaz ME, Eisner DA. Stimulation of Ca-induced Ca release only transiently increases the systolic Ca transient: measurements of Ca fluxes and sarcoplasmic reticulum Ca. *Cardiovasc Res*. 1998;37(3):710-717.
46. Dumitrescu C, Narayan P, Efimov IR, et al. Mechanical alternans and restitution in failing SHHF rat left ventricles. 2002;282(4):H1320-H1326.
47. Vittone L, Mundiña-Weilenmann C, Said M, Ferrero P, Mattiazzi A. Time course and mechanisms of phosphorylation of phospholamban residues in ischemia-reperfused rat hearts. Dissociation of phospholamban phosphorylation pathways. *J Mol Cell Cardiol*. 2002;34(1):39-50.
48. Petroff MG, Aiello EA, Palomeque J, Salas MA, Mattiazzi A. Subcellular mechanisms of the positive inotropic effect of angiotensin II in cat myocardium. *J Physiol*. 2000;529 Pt 1(Pt 1):189-203.
49. Aiello EA, Villa-Abrille MC, Escudero EM, et al. Myocardial hypertrophy of normotensive Wistar-Kyoto rats. *Am J Physiol Heart Circ Physiol*. 2004;286(4):H1229-1235.
50. Prosser BL, Ward CW, Lederer WJ. X-ROS signaling: rapid mechano-chemo transduction in heart. *Science (New York, NY)*. 2011;333(6048):1440-1445.
51. Sommese LM, Racioppi MF, Shen X, et al. Discordant Ca(2+) release in cardiac myocytes: characterization and susceptibility to pharmacological RyR2 modulation. *Pflugers Archiv : European journal of physiology*. 2022;474(6):625-636.
52. Pasqualin C, Gannier F, Malécot CO, Bredeloux P, Maupoil V. Automatic quantitative analysis of t-tubule organization in cardiac myocytes using ImageJ. *American journal of physiology Cell physiology*. 2015;308(3):C237-245.
53. Frisk M, Norseng PA, Stenersen Espe EK, Louch WE. Tubulator: an automated approach to analysis of t-tubule and dyadic organization in cardiomyocytes. *Philosophical transactions of the Royal Society of London Series B, Biological sciences*. 2022;377(1864):20210468.

FIGURE LEGENDS

Figure 1. Rate-dependent mechanical alternans in W and SHR perfused hearts. A) Representative left ventricular developed pressure (LVDP) recordings from W and SHR perfused hearts at 3, 6 and 12 mo of age at 4 Hz (basal) and 8.5 Hz. B) Average mechanical alternans ratio (AR) obtained by increase in stimulation frequencies (4 to 11 Hz) ($n = 4-6$ hearts). * $P < 0.05$ vs. age-matched W at the same frequency calculated by two-tailed Student's T-test.

Figure 2. Rate-dependent Ca^{2+} alternans in W and SHR myocytes. A) Typical cytosolic Ca^{2+} transients recordings of 12 mo W and SHR myocytes stimulated at progressively greater frequencies. B) Overall results of threshold pacing frequency to induce Ca^{2+} alternans in 3, 6 and 12 mo W and SHR myocytes ($n = 7-30$, from 2-5 hearts). * $P < 0.05$ vs. age-matched W. All groups were compared by one-way ANOVA followed by Newman-Keuls test.

Figure 3. Subcellular Ca^{2+} alternans. A) Typical confocal line-scan images of cytosolic Ca^{2+} transients and intensity profiles of 12 mo W (up) and SHR (down) myocytes stimulated at 1 and 4 Hz. B) Overall results of discordant index (DI) measured at 4 Hz in 12 mo W and SHR myocytes ($n = 9-11$ cells, 3-4 hearts). * $P < 0.05$ vs. W calculated by unpaired Student's T-test.

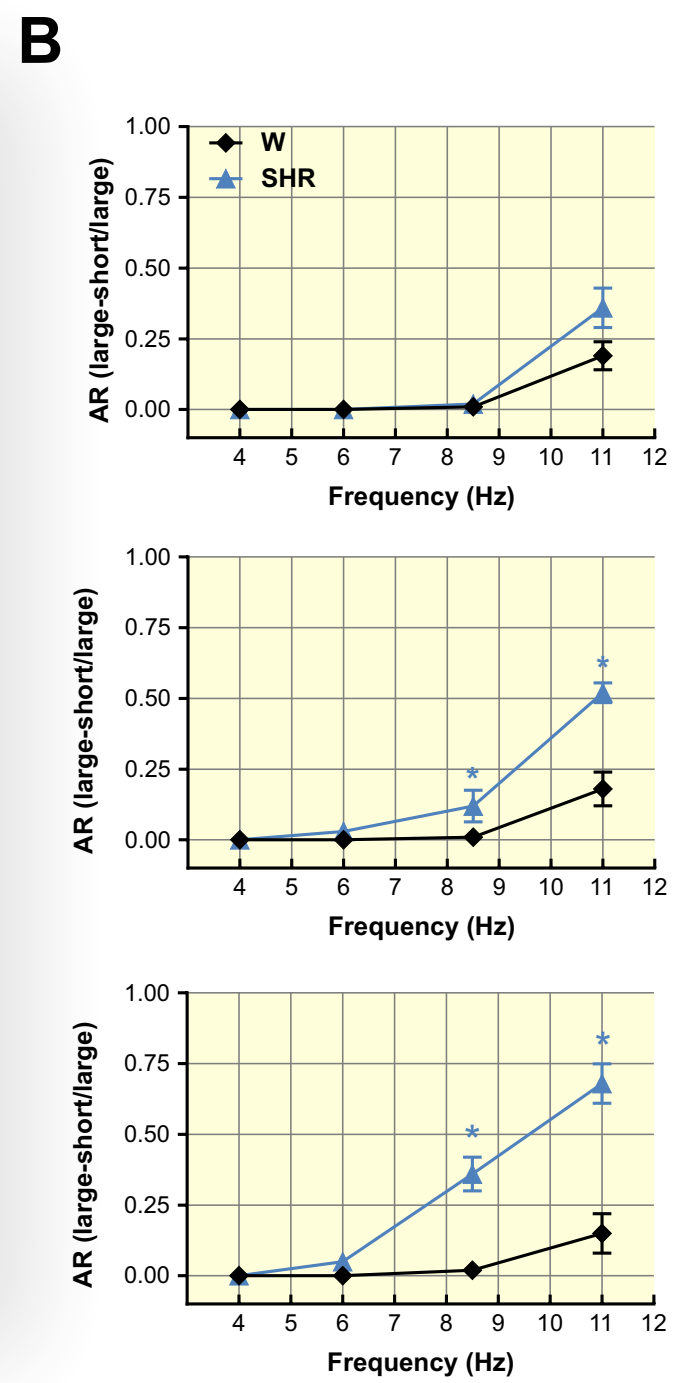
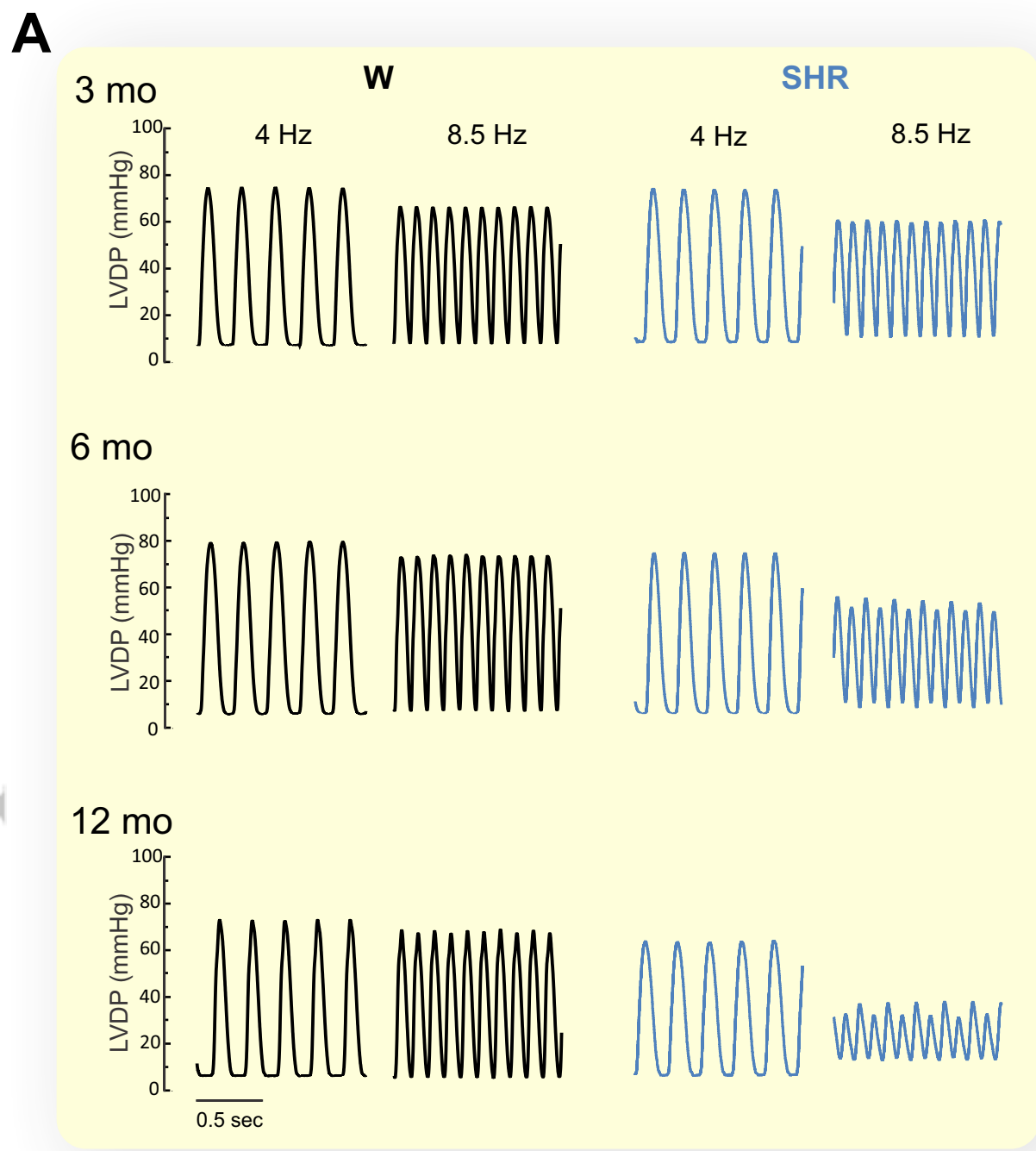
Figure 4. T-Tubule organization. A) Typical confocal images of 6 mo W and SHR myocytes stained with Di-8-ANNEPS. B) Average results of the index of TT regularity (TT power) in 6 mo W and SHR myocytes ($n = 18-33$ cells, from 2-4 rats). C) Overall results of transverse and longitudinal T-tubule expressed as percentage of all T-tubule. * $P < 0.05$ vs. W calculated by unpaired Student's T-test.

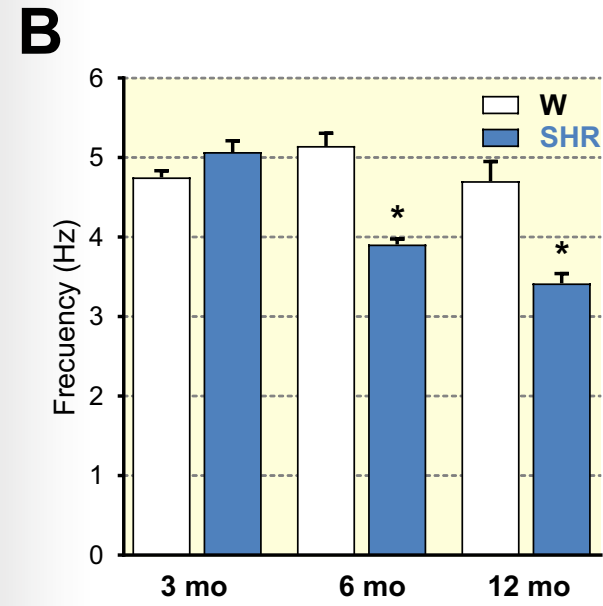
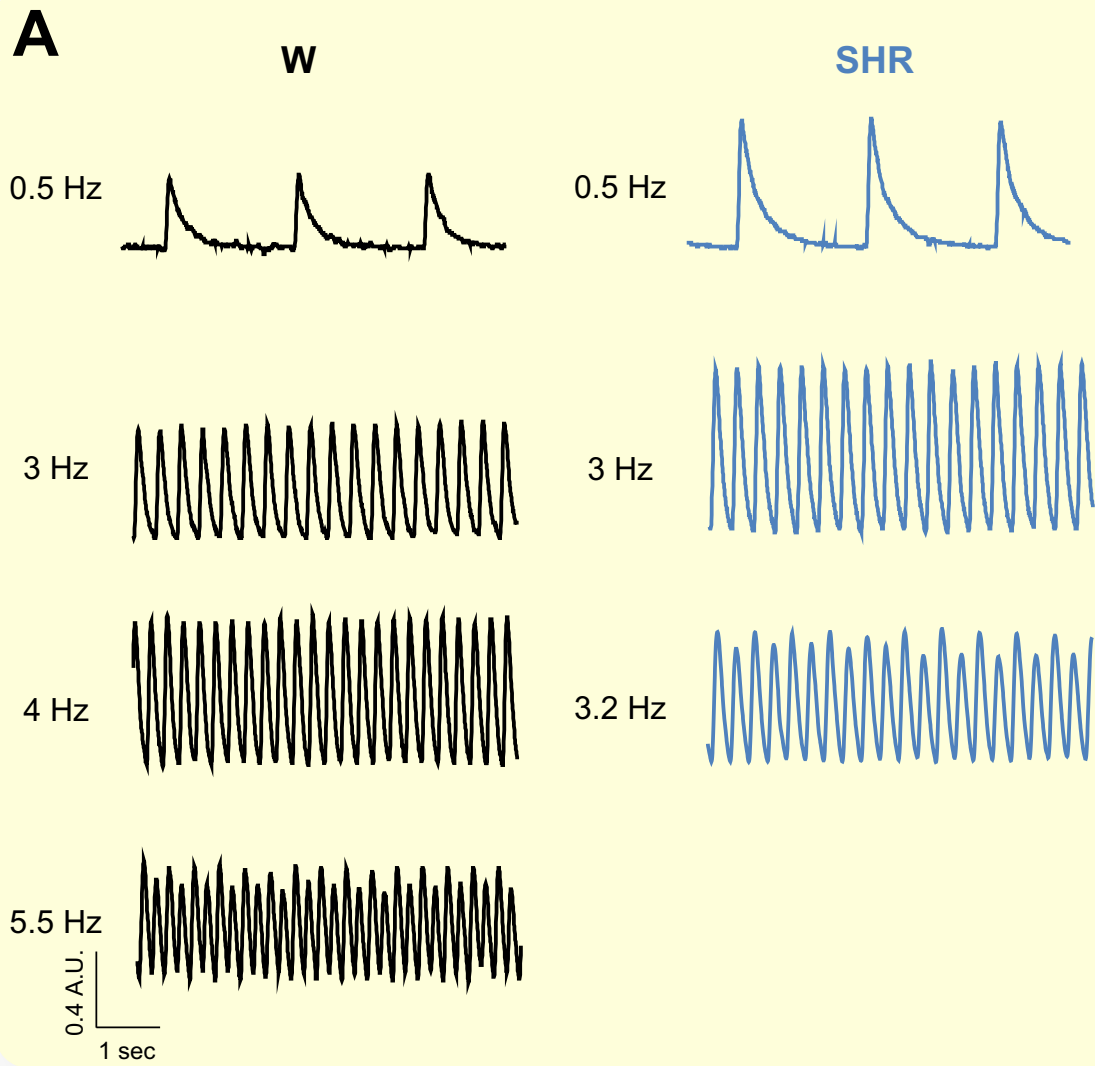
Figure 5. Evaluation of SR Ca^{2+} uptake in W and SHR myocytes. A) Representative superimposed Ca^{2+} transient traces of 12 mo W and SHR myocytes at 0.5 Hz (solid line) and 3 Hz (dashed line). B) Overall results of the time constant of single exponential decay of Ca^{2+} transient (τ) at 0.5 and 3 Hz in 6 and 12 mo W and SHR myocytes ($n = 13-20$ cells, from 3-4 hearts). * $P < 0.05$ vs. 0.5 Hz calculated by paired Student's T-test.

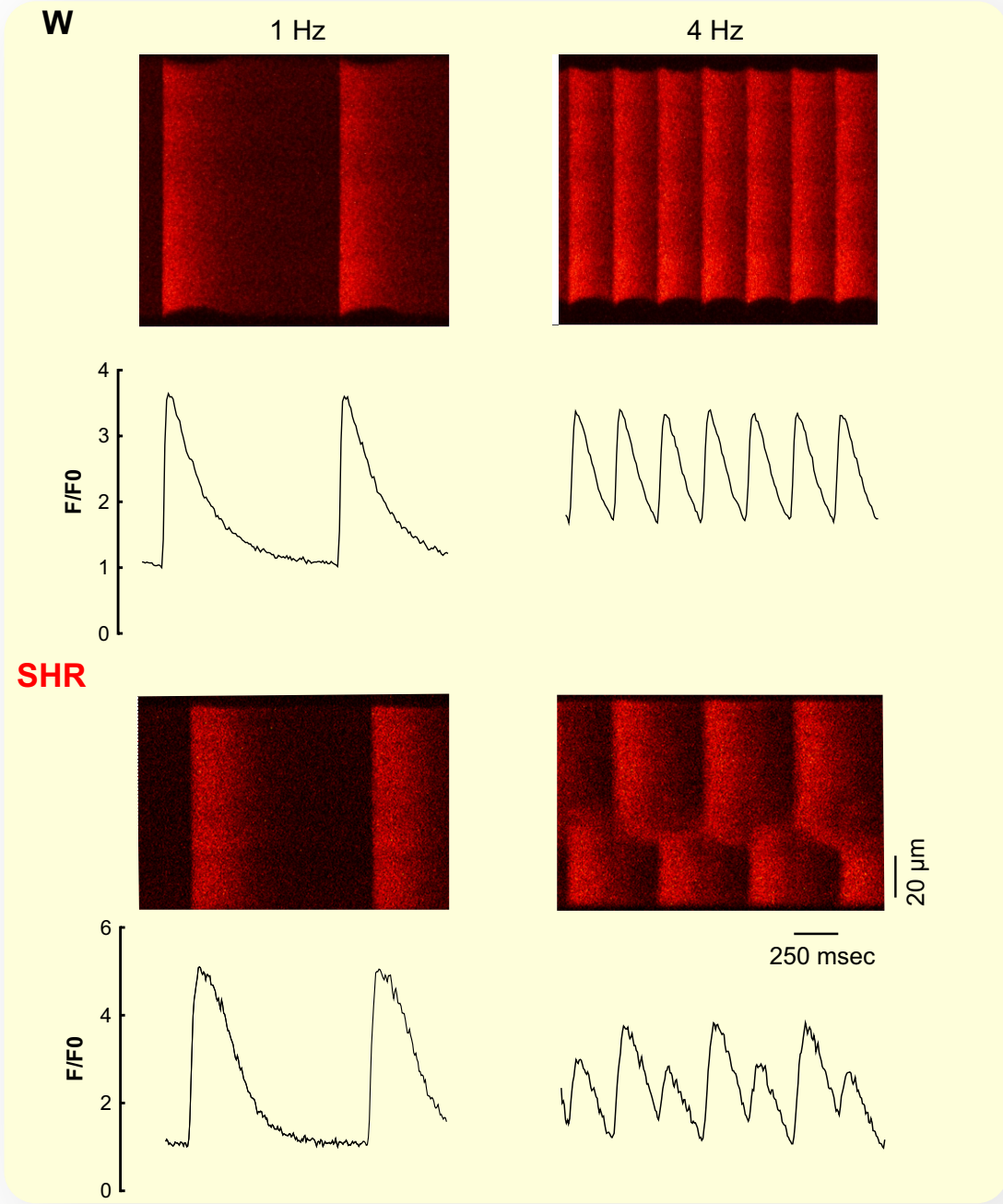
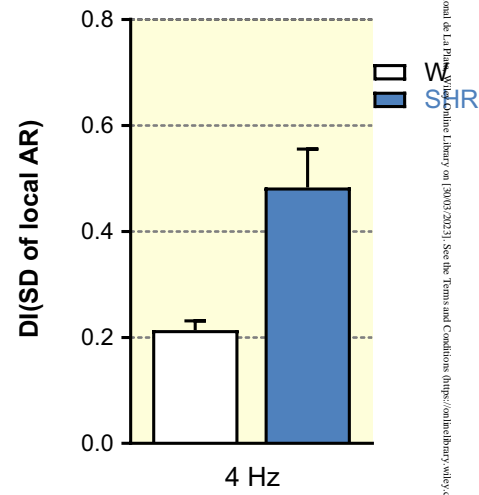
Figure 6. Restitution of Ca^{2+} release in W and SHR myocytes. A) Typical Ca^{2+} transient recorded in 6 mo W and SHR myocytes in response to the experimental protocol shown in W: additional stimulation pulses (S2) were

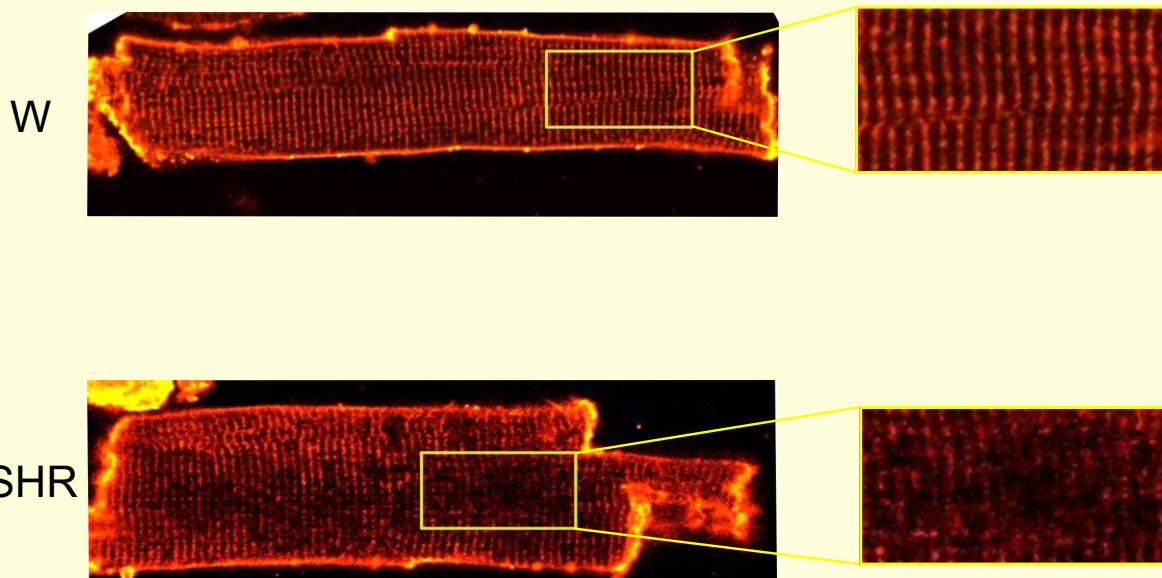
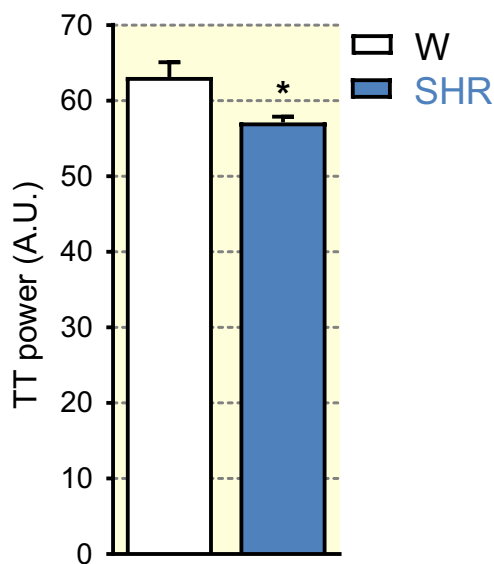
applied at different times with respect to the regular pulse (S1) and their respective amplitudes (A2 and A1) were used to calculate the fractional recovery. B) Average restitution of Ca^{2+} release curves, obtained by plotting fractional recovery ($\%A2/A1$) at different S1-S2 intervals, in 6 mo W, SHR and SHR myocytes treated with low doses of caffeine (100 μM , caff). C) Time interval to 50% of recovery of Ca^{2+} transients of the same cells ($n = 10-30$ cells from 2-5 rats). * $P < 0.05$ vs. W, # $P < 0.05$ vs. SHR. One-way ANOVA followed by Newman-Keuls test was used for analysis. D) Typical alternating cytosolic Ca^{2+} transients recordings of SHR myocytes before and after caff treatment. E) Overall results of AR in SHR myocytes with or without caff treatment ($n = 5$ cells from 4 rats). * $P < 0.05$ vs. SHR before caff treatment. Paired Student's T-test was used for analysis.

Figure 7. Effects of increased extracellular Ca^{2+} concentration on Ca^{2+} alternans. A) Representative traces of caffeine-induced Ca^{2+} transient to evaluate SR Ca^{2+} load in 6 mo SHR myocytes at 1 mM and 2.5 mM extracellular Ca^{2+} concentrations. B) Summary data for the amplitude of caffeine-induced Ca^{2+} transients of the same groups as an indicator of SR Ca^{2+} content ($n = 7-9$ cells, from 2-3 hearts). * $P < 0.05$ vs. 1 mM Ca^{2+} analyzed by paired Student's T-test. C) Average restitution of Ca^{2+} release curves from 6 mo SHR myocytes at 1mM or 2.5 mM Ca^{2+} . * $P < 0.05$ vs. 1 mM Ca^{2+} analyzed by paired Student's T-test. D) Time interval to 50% of recovery of Ca^{2+} transients of the same cells ($n = 5-6$, from 2 hearts). * $P < 0.05$ vs. 1 mM Ca^{2+} . E) Typical cytosolic Ca^{2+} transient recordings of 6 mo SHR myocytes at high pacing frequency to induce alternans showing the effects of superfusion of 2.5 mM Ca^{2+} . F) Overall results of AR in 6 mo SHR myocytes at 1 mM and 2.5 mM extracellular Ca^{2+} concentrations ($n = 9$ cells, from 3 hearts). * $P < 0.05$ vs. 1 mM Ca^{2+} analyzed by paired Student's T-test.





A**B**

A**B****C**